European Journal of Immunology Clinical·Basic·Translational

New Technology

Basic

Research Article

An induced thymic epithelial cell-based high throughput screen for thymus extracellular matrix mimetics

Paul Rouse[1], *Timothy Henderson*[1,3], *Seshasailam Venkateswaran*[2], *Joanna Sweetman*[1], *Cairnan Duffy*[2], *Mark Bradley*[2] *and C. Clare Blackburn*[1]

[1] Centre for Regenerative Medicine, School of Biological Sciences, Institute for Stem Cell Research, 5 Little France Drive, Edinburgh, EH16 4UU, UK
[2] School of Chemistry, University of Edinburgh, Joseph Black Building, Edinburgh, EH8 9YL, UK
[3] Australian National University Medical School, The Canberra Hospital, Garran, ACT 2605, Australia

Thymic epithelial cells (TECs) are key effectors of the thymic stroma and are critically required for T-cell development. TECs comprise a diverse set of related but functionally distinct cell types that are scarce and difficult to isolate and handle. This has precluded TEC-based screening assays. We previously described induced thymic epithelial cells (iTECs), an artificial cell type produced *in vitro* by direct reprogramming, raising the possibility that iTECs might provide the basis for functional screens related to TEC biology. Here, we present an iTEC-based three-stage medium/high-throughput *in vitro* assay for synthetic polymer mimics of thymic extracellular matrix (ECM). Using this assay, we identified, from a complex library, four polymers that bind iTEC as well as or better than gelatin but do not bind mesenchymal cells. We show that these four polymers also bind and maintain native mouse fetal TECs and native human fetal TECs. Finally, we show that the selected polymers do not interfere with iTEC function or T-cell development. Collectively, our data establish that iTECs can be used to screen for TEC-relevant compounds in at least some medium/high-throughput assays and identify synthetic polymer ECM mimics that can replace gelatin or ECM components in TEC culture protocols.

Keywords: cellular reprogramming · epithelial cells · extracellular matrix · high throughput screening assays · thymus

Additional supporting information may be found online in the Supporting Information section at the end of the article.

Introduction

The thymus is the primary lymphoid organ responsible for generating and shaping the T-cell repertoire. The process of T-cell repertoire development, called thymopoiesis, depends on dynamic interactions between developing T cells (thymocytes)

Correspondence: C. Clare Blackburn
e-mail: c.blackburn@ed.ac.uk

and the thymic stroma. The main functional element of the stroma, the thymic epithelium, comprises several related but functionally distinct thymic epithelial cell (TEC) types that collectively mediate T-cell lineage commitment, development and repertoire selection [1].

TECs constitute less than one percent of total adult thymic cellularity and are fragile cells that are difficult to isolate and work with *ex vivo*. This has precluded the development of medium/high throughput screens for modulators of TEC functionality. Indeed, to date, investigation of thymus biology *in vitro* has relied on the necessarily low throughput techniques of fetal thymic and reaggregate fetal thymic organ culture (FTOC and RFTOC, respectively) [2–4] and on the OP9-DLL1 and MS5-hDLL1 cell line-based systems that partially support thymopoiesis but do not support physiological T-cell repertoire selection [5–14]. None of these models are suitable for high-throughput screening relevant to TEC-dependent thymus functions. We have previously shown that overexpression of the transcription factor Forkhead Box N 1 (FOXN1) in murine embryonic fibroblasts (MEFs) results in conversion of MEFs into 'induced thymic epithelial cells' (iTECs), which closely mimic TECs in terms of phenotype and function [15]. This led us to ask whether iTEC could provide the basis for TEC-relevant medium/high-throughput screening assays.

Biocompatible synthetic polymers that provide chemically defined substrates for the *in vitro* expansion of specific cell types have previously been described [16–18] and can reduce the batch-to-batch variation associated with naturally occurring substrates such as gelatin and Matrigel [19]. Synthetic polymers that support TECs in culture have not, however, been reported, with previous studies focusing on the use of fabricated tantalum-coated [20] or natural thymic extracellular matrix (ECM) scaffolds [21–26]. We therefore devised and tested a three-tier iTEC-based medium/high-throughput screening assay designed to select, from a large synthetic polymer library, polymers that could specifically support functional TECs *in vitro*.

Using this assay, we identified four polymers that bind and support iTECs as well as or better than gelatin but do not bind MEFs in monolayer culture. We showed that, in addition to iTECs, these polymers could support native mouse fetal TECs and native human fetal TECs *in vitro*. We further demonstrated that iTECs cultured on these substrates are functional, as evidenced by their ability to mediate T-cell development *in vitro*. Collectively, our findings validate iTEC as a tool for higher throughput screening approaches related to mouse and human TEC biology, pointing to the potential for further developments in this area. Additionally, they provide a further step toward the identification of fully defined conditions for culturing TECs *in vitro*.

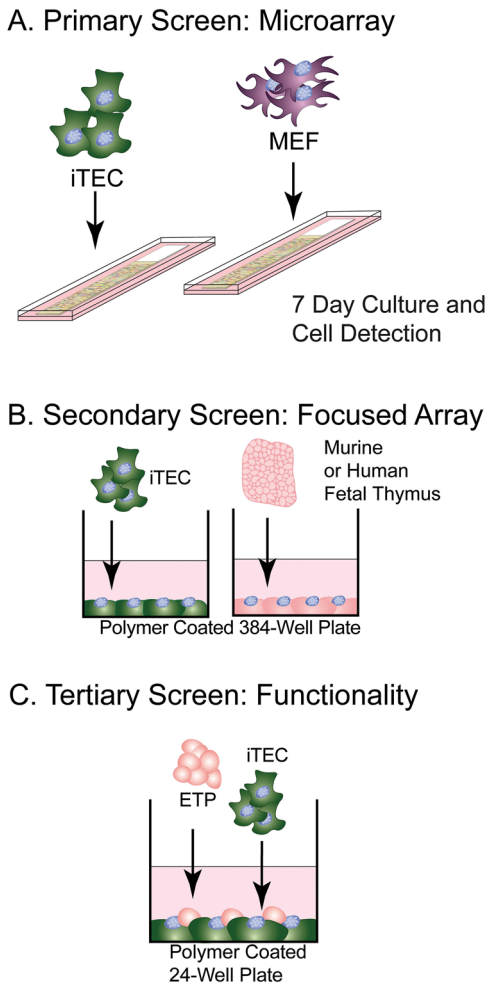

Figure 1. Schematic representation of the three-stage screening assay for selection, from a library, of polymers with the capacity to bind and support functional TECs *in vitro*. (A) Primary screen: polymer microarrays produced by contact printing of 334 individual synthetic polymers were screened separately with TEC and MEFs. Each polymer was represented in quadruplicate on each microarray. (B) Secondary screen: polymers selected in the primary screen were tested in a fully automated 384-well plate-based screening assay for their capacity to bind iTECs, fetal mouse, and fetal human TECs. (C) Tertiary screen: iTECs were cocultured with ETPs on each of the polymers that bound all three cell types and assayed to ensure that these polymers did not negatively affect iTEC-mediated T-cell development.

Results

Primary screen: Identification of synthetic polymers that support induced thymic epithelial cells

The minimal requirements for a polymer to be suitable for use in cell culture are that it promotes adhesion and survival of the target cell type and does not interfere with the functionality of the cell type in question. Our primary screen was therefore designed to identify polymers that selectively bound TEC from a complex synthetic polymer library, with the secondary screen validating and extending the results from the primary screen and the tertiary screen testing for interference with cell type functionality (Fig. 1). We employed iTECs as a substitute for native TECs in the primary screen since iTECs exhibit key phenotypic and functional attributes of TECs (Figs. S1 and S2) [15], and in contrast to native TECs, iTEC numbers are not limiting.

In brief, a library of 334 different synthetic polymers was generated as previously described [19]. The library included polymer compositions that encompassed a range of physical

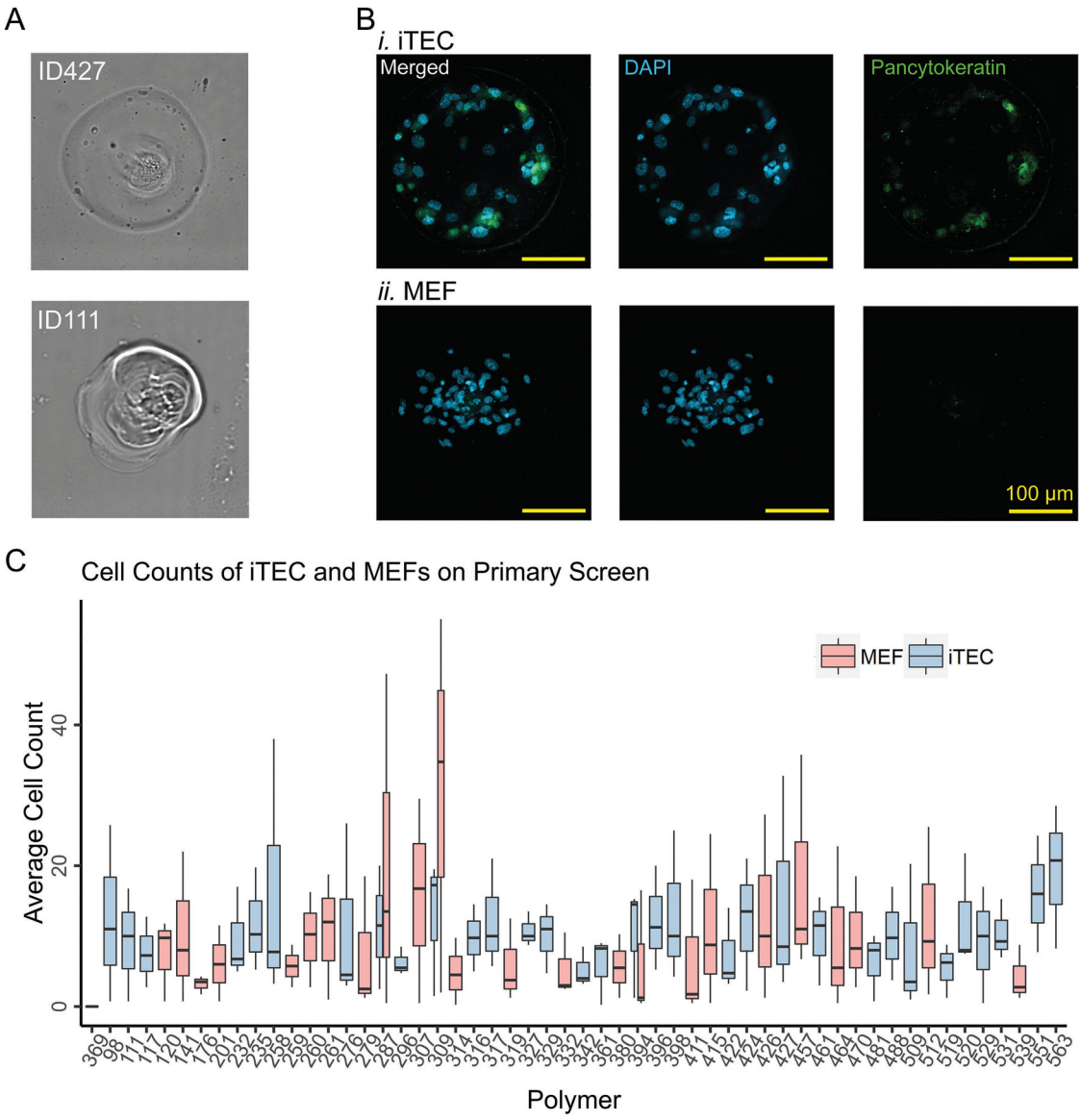

Figure 2. Primary screen identifies synthetic polymers able to support iTECs, MEFs or both cell types. (A) Brightfield images of contacted printed polymer spots in the microarray. Images show spots of polymers ID427 (top) and ID111 (bottom) in the absence of cells. (B) Representative images of iTECs (Bi. top) or MEFs (Bii. bottom) present on individual polymer spots after 7 days of culture. DAPI identifies nuclei and was used to count the number of cells on each spot; α-pancytokeratin (panK) identifies iTECs. (C) Boxplot shows the number of iTECs or MEFs present on each polymer type after 7 days of culture. Polymers that had no cells attached are not shown with the exception of Polymer ID369, which is used as a no-binding control in downstream experiments. n = 3 independent biological replicates, each with four technical replicates. Plots were formatted as box and whisker, and no statistical analysis was performed.

properties, including different functional groups, wettability, charge, nanotopography, integrin contact point density and lipophilicity [19, 27, 28]. To produce the primary screen, microscope slides were coated in 2% agarose to prevent cell adhesion to the glass, and the individual members of the polymer library were contact printed onto this slide such that each polymer was represented in quadruplicate, creating a matrix of polymer spots [19]. Two representative individual spots are shown in Fig. 2A. The slides were then seeded with 2×10^5 iTECs in 1 ml of medium and placed into culture (see Fig. S1 for gating strategy for GFP^+ iTECs). Negative controls were provided by 4-hydroxytamoxifen (4OHT)-treated *Rosa26*$^{CreERT2/+}$ MEFs. These cells controlled for cell-type specificity and for any nonspecific effects of the CreERt2 fusion protein.

After seven days of culture, the slides were stained with DAPI and anti-pancytokeratin (panK; a marker of epithelial cells not expressed by MEFs) (Fig. 2B). They were then screened by high-content imaging, and the number of cells on each polymer spot was determined (Fig. 2C). Polymer spots were scored positive if either iTECs ($panK^+$ cells), MEFs ($panK^-$ cells), or both cell types were present on all four technical replicates in all three independent experiments. Using these criteria, thirty-two of the three

hundred thirty-four polymers tested bound iTEC (ID98, 111, 117, 232, 235, 258, 276, 287, 296, 309, 316, 317, 327, 329, 342, 361, 394, 396, 398, 422, 424, 427, 461, 481, 488, 509, 519, 520, 529, 531, 551, 563), while twenty-four bound MEFs (ID120, 141, 176, 201, 259, 260, 261, 279, 287, 307, 309, 314, 319, 332, 380, 394, 411, 415, 426, 457, 464, 470, 512, 539) (Fig. 2D). There was minimal overlap between the polymers that bound iTEC and those that bound MEFs, with only polymers ID287, 309, and 394 binding both cell types (Fig. 2D).

Secondary screen: Automated screening of a focused polymer array

The thirty-two polymers identified as binding iTEC in the primary screen (including polymers that bound both iTEC and MEFs) were taken forward for further investigation in a focused secondary screen that required lower input cell numbers. This screen was used to assess iTEC binding and maintenance on the polymers more quantitatively and to test the capacity of the polymers that bound iTEC to bind native mouse and human TEC.

In brief, the secondary screen was performed in 384-well plates and used automated liquid handling and imaging to reduce within-screen variance and thus to identify differences in iTEC/TEC-binding capacity between polymers. The test polymers were coated onto individual wells of 384-well plates (see Materials and Methods). Polymers ID117, 232, 235, 276, 296, 317, 329, I42, 422, 424, 461 and 488 either did not dissolve in acetone or produced a highly autofluorescent layer following solvent casting and were excluded from this array, leaving twenty polymers included in the secondary screen. Positive and negative controls were provided by wells coated with gelatin and wells coated with polymer ID369, which bound MEF but not iTEC in the primary screen, respectively. iTECs, native mouse fetal TECs, or native human fetal TECs were seeded into the arrays (see Materials and Methods), and at the experimental end-point, the arrays were fixed and processed for analysis by staining with DAPI and panK (Figs. 3A, B).

For analysis, we used Columbus software (Perkin Elmer) to create a pipeline that identified the number of epithelial cells ($panK^+$ cells) and the total number of cells ($DAPI^+$ cells) in each well, as follows. We first separated each 384-well plate into twenty fields of view and segmented each nucleus ($DAPI^+$ area) to calculate the total number of cells. The area surrounding each nucleus was then segmented into individual cells using cellular autofluorescence (note that this required a camera with a high bit depth). Areas with variable brightness with respect to the neighboring region were delineated and assumed to mark the boundary between cells, thereby pairing a nucleus with a surrounding delineated area corresponding to cytoplasm to create a whole cell. To determine the number of iTECs in each well, the mean fluorescence intensity (MFI) in the panK-AF488 channel was calculated for each 'cell' (i.e., each delineated area extending from a $DAPI^+$ spot), and this was used to parse the cells into two populations (Fig. 3C, depictions of input (upper) and output (lower)). A constant MFI threshold, set qualitatively although visual back testing, was used to select the $panK^{hi}$ population for each experiment rather than recalculating the threshold for each field of view. As the largest source of variation between independent experiments was accounted for by variation in the input cell number (likely arising from errors in the cell counts generated during flow cytometric cell sorting), between-experiment variation was normalized by reporting each cell count divided by the cell count on gelatin for each experiment (see Figs. S3 and S4 for details of the normalization strategy in the iTEC and TEC arrays, respectively).

The number of $panK^{hi}$ cells present on each polymer was then determined. Most of the polymers in this secondary screen bound all three TEC populations tested (Fig. 3D). However, the cell numbers bound per well varied dramatically between polymers, and therefore, to identify polymers to take forward for further study, we compared the number of $panK^{hi}$ cells bound to each polymer to the number bound to the negative control polymer ID369. Polymers ID111, 287, 427, 519 and 563 all bound and maintained equivalent or higher numbers of $panK^{hi}$ iTECs than wells coated with gelatin and bound significantly higher numbers of $panK^{hi}$ iTECs than wells coated with the negative control polymer ID369 (Fig. 3D; Table 1). These polymers all also bound native mouse and native human fetal TECs, and with the exception of ID563, similar numbers of cells were present for all three TEC populations tested (Fig. 3D; Table 1). Polymer ID394, which bound both iTECs and MEFs in the primary screen, bound iTECs but with fewer cells present in each well and bound mouse and human fetal TECs (Fig. 3D; Table 1). In addition to these polymers, native human fetal TEC bound polymers ID258, 309, 396, 520 and 531 (Fig. 3D; Table 1), which did not bind and maintain iTEC as efficiently as gelatin in the secondary screen. Only Polymer ID287 bound MEFs, iTECs, mouse fetal TECs and human fetal TECs.

Chemical composition of polymers selected by the screen

The above experiments identified four polymers (ID111, 287, 427 and ID519) that supported iTEC, native mouse and native human TEC, and two additional polymers, ID394 and 563, that bound native mouse TEC, as well as or better than gelatin. Polymers ID394 and 563 also bound iTECs and human TECs but with fewer cells from these populations bound than from native mouse TECs. The composition of these six polymers and the structures of their monomer components are shown in Table 2 and Fig. 4, respectively. The principal monomer in polymers ID111, 287, 427, 519 and 563 was methoxyethyl methacrylate (MEMA), while ID394 was principally ethyl methacrylate (EMA). We note that not all MEMA-based polymers were able to bind and maintain iTECs, and not all EMA-based polymers were able to bind native mouse TECs. As examples, polymer ID394 (EMA 70%, DEAEMA 30%) bound native TEC as well as gelatin, while Polymer ID398 (EMA 50%, DEAEA 50%) did not (Fig. 3D).

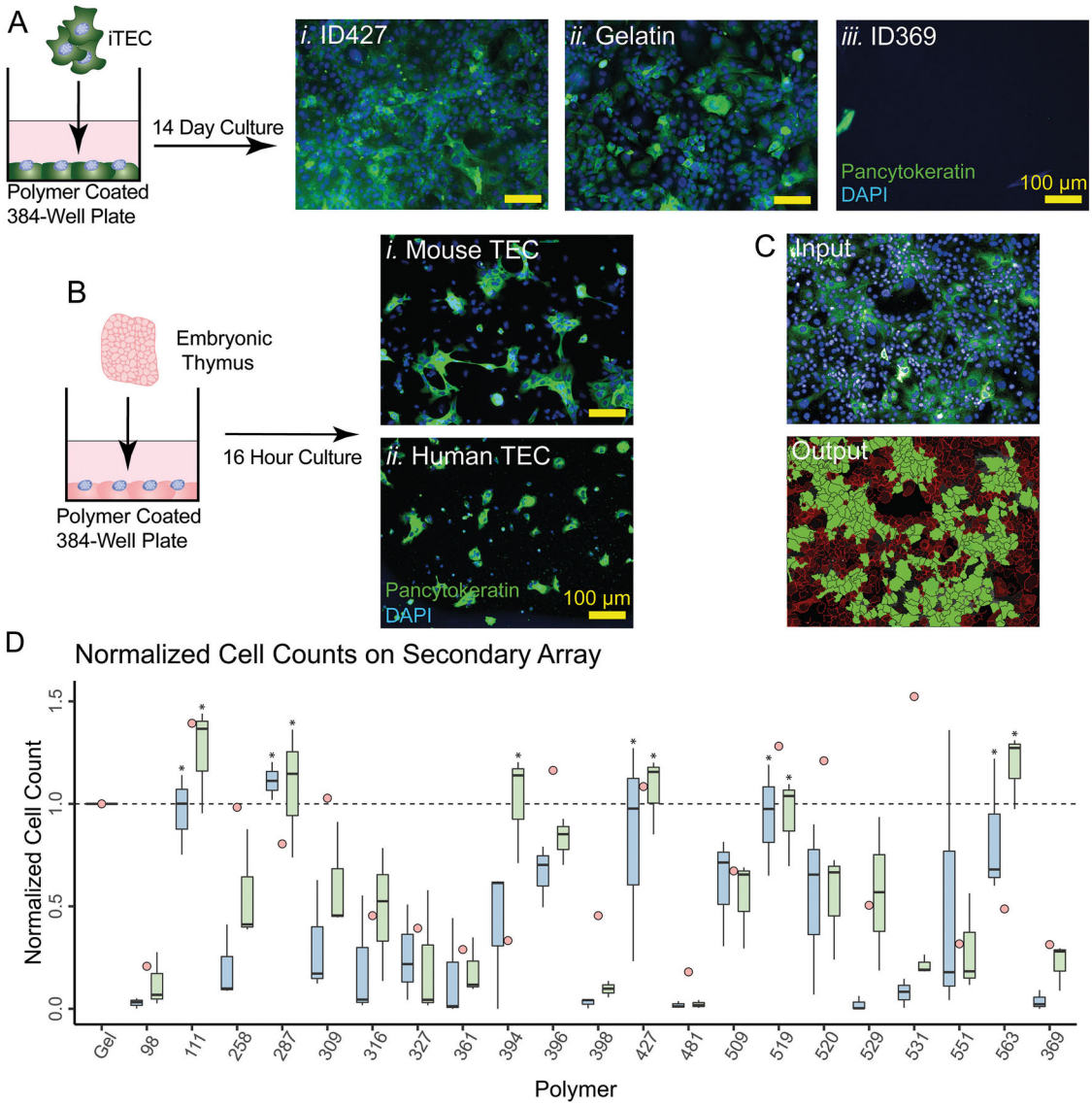

Figure 3. An automated secondary screen identifies five polymers able to bind and support iTECs, native mouse fetal TECs and native human fetal TECs. (A) A focused array of the 20 polymers selected in the primary screen and compatible with solvent casting was produced by coating individual polymers onto wells of a 384-well plate. iTECs were seeded into each well, cultured for 14 days, and then stained with α-pancytokeratin (panK) and DAPI. Images show representative fields of view of *(i)* polymer ID427, *(ii)* gelatin (Gel; positive control) and *(iii)* polymer ID369 (negative control). (B) Single-cell suspensions of E13.5/E14.5 mouse thymus or week 11 human fetal thymus cells were cultured for 16 hours on individual polymers in the focused array. Images show representative wells for mouse or human thymi cultured in gelatin-coated wells after staining with panK and DAPI. (C) Depiction of the image analysis pipeline wherein the top panel shows the input image and the bottom depicts the output. (D) Plot shows the number of all three cell types observed on each polymer normalized to the count in wells coated with 0.1% gelatin (*left*). Blue, iTEC; Red, human fetal TEC; Green, mouse fetal TEC. Levene's and Shapiro–Wilk tests established equal variances and normality, respectively. One-way ANOVA followed by Dunnett's comparisons test compared each polymer to polymer ID369. * p value < 0.05. iTEC: n = 3 independent biological replicates, each with three technical replicates; human TEC: n = 1 biological sample with one technical replicate; murine TEC: n = 3 independent biological replicates, each with one technical replicate. Plots formatted as box and whisker.

Tertiary screen: Functionality of iTECs cultured on the lead candidate polymers

As a final step, we designed a tertiary screen to test whether culture on each of the four polymers (ID111, 287, 427 and 519) interfered with the ability of iTEC to support thymocyte development. For this, we used a low-throughput assay in polymer-coated 24-well plates (one polymer per well), in which iTECs were cocultured with adult early thymic progenitors (ETPs) for 14 days (Fig. 5A, Fig. S5), after which αβ T-cell development was assayed by flow cytometric analysis of CD4/CD8 thymocyte subset distribution (gating strategy shown in Fig. S6).

After 14 days of coculture, small round cells were microscopically visible on the surface of the iTEC monolayers in all wells, consistent with the presence of T cells (Fig. 5B). Analysis of subset distribution based on CD4 and CD8 staining (Fig. 5C) revealed

Table 1. Capacity of the polymers selected in the primary and secondary screens to bind iTECs, mouse fetal TECs and human fetal TECs. For iTECs and mouse fetal TECs, the polymers shown are those that bound significantly more cells than those bound by polymer ID369; for human fetal TEC polymers that bound significantly more cells than those bound by gelatin are shown. The exception is ID287, which bound low numbers of human TECs. $p > 0.05$, $\alpha = 0.05$

		Cell type assayed for polymer binding		
		iTEC	Mouse fetal TEC	Human fetal TEC
Polymer ID	**111**	+	+	+
	287	+	+	+ (weakly)
	427	+	+	+
	519	+	+	+
	563	+	+	–
	394	–	+	–
	309	–	–	+
	396	–	–	+
	520	–	–	+
	531	–	–	+

the presence of $CD4^-CD8^-$ double negative (DN), $CD4^+CD8^+$ double positive (DP), and $CD4^+CD8^-$ and $CD4^-CD8^+$ single positive (SP4 and SP8, respectively) thymocyte populations in wells coated with each of the six polymers, with most polymers performing as well as gelatin or Matrigel (Fig. 5D). Although not statistically significant, wells coated with polymer ID427 appeared to contain higher numbers of DP, SP4 and SP8 cells than wells coated with the other polymers or gelatin (Fig. 5E) or Matrigel. From the 5,000 initial input ETPs, the wells in which iTECs were cultured on polymer ID427 produced an average of 15,749 DN, 500 DP, 273 SP4 and 508 SP8 thymocytes, while iTECs cultured on gelatin produced an average of 8,306 DN, 386 DP, 206 SP4 and 389 SP8 thymocytes. As a suitable method for normalization between independent experiments was not identified, the between-experiment variation found in the counts of DN, DP, SP4 and SP8 thymocytes generated on each polymer was considered. Polymer ID427 exhibited the lowest mean coefficient of variation (CoV) between all polymer counts and was therefore considered to be the best material to satisfy the criteria of being able to bind native mouse and human fetal TEC and iTEC and of reducing experiment-to-experiment variation (Table S7). Importantly, the data obtained from Polymer ID427 demonstrate that a synthetic, defined substrate can replace natural substrates, including gelatin, with no loss in function.

Culture on polymer ID427 results in increased MHC Class II Expression on iTEC

The trend for the production of increased numbers of SP4 in wells coated with polymer ID427 suggested that this polymer directly or indirectly promoted iTEC functionality and/or expression of MHC Class II (MHCII) on iTECs (Fig. 5D). We therefore tested the expression of the MHCII gene *H2-Eb1* in iTECs after coculture with ETPs for 14 days. iTECs cultured on polymer ID427 and Matrigel had higher levels of *H2-Eb1* expression than freshly isolated iTECs (i.e., iTEC prior to coculture; Fig. 6A*i*, *ii*, $p = 0.02$ and $p = 0.9$, respectively), indicating that culture on polymer ID427 was as good as Matrigel with respect to this important parameter.

In addition, we analyzed the expression of a panel of genes encoding proteins required for TEC function: FOXN1 (*Foxn1*), the master regulator of TEC differentiation and transgene

Table 2. List of polymerizable monomers and amines used in the synthesis of the polymers that bound iTEC and native mouse and human fetal TEC in the secondary screen. This table details the monomer composition of the selected polymers, with structures given in Fig. 4

		Polymer composition			
		Monomer 1 (ratio)	Monomer 2 (ratio) Group	Monomer 3 (ratio) Group	Molecular Weight
Polymer ID	**111**	MEMA (90%)	BAEMA (10%) Amine	–	273,000
	287	MEMA (50%)	GMA (50%) Amine	MAn (>1%) Amine	>2,000,000
	309	MMA (90%)	GMA (10%) Amine	DnHA (>1%) Amine	1,900,000
	394	EMA (70%)	DMAEMA (30%)	–	120,000
	396	EMA (90%)	DEAEA (10%) Amine	–	123,000
	427	MEMA (60%)	DEAEA (10%) Amine	BMA (30%) Amine	111,000
	519	MEMA (60%)	DEAEMA (10%) Amine	St (30%) St	86,600
	520	MEMA (60%)	DEAEMA (30%) Amine	St (10%) St	143,000
	531	MEMA (55%)	DEAEMA (45%) Amine	–	141,000
	563	St (75%)	GMA (30%) Amine	–	–

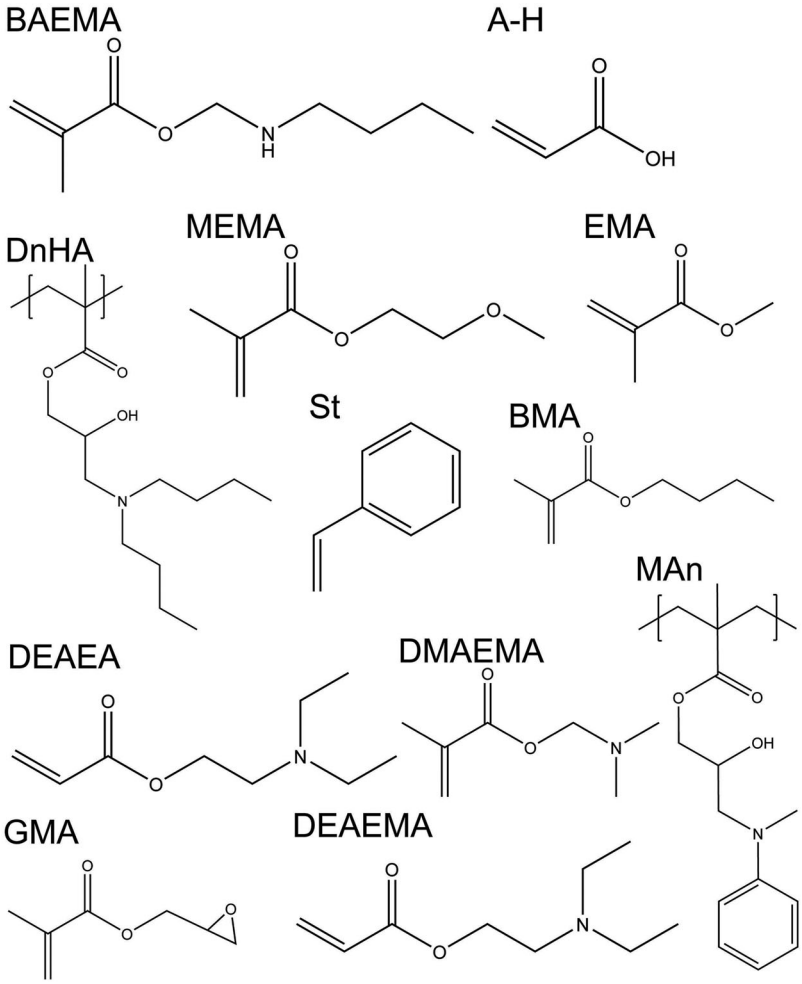

Figure 4. Chemical structures of the polymer building blocks: Diagrams show monomers used to fabricate the polymers identified as supporting TEC in the secondary screen. MEMA (2-methoxyethyl methacrylate); EMA (ethyl methacrylate); BAEMA (2-(tert-butylamino)ethyl methacrylate); GMA (glycidyl methacrylate); DMAEMA (2-(dimethylamino)ethyl methacrylate); DEAEA (2-(diethylamino)ethyl acrylate); MAn (N-methylaniline); BMA (butyl methacrylate); DEAEMA (2-(diethylamino)ethyl methacrylate); St (styrene), A-H (acrylic acid), DnHA (di-n-hexlyanmine) (see also Table 2 and Table S4).

driving iTEC identity [15]; Delta-like 4 (*Dll4*), the nonredundant ligand for T-cell lineage commitment [29, 30]; the immunoproteasome subunit β5t (encoded by *Psmb11)* and protease cathepsin L (*Ctsl1*), both expressed specifically in cTECs and essential for the production of normal $CD8^+$ and $CD4^+$ T-cell repertoires, respectively [8, 31]; chemokine (C-C motif) ligand 25 (*Ccl25*), responsible for colonization of the thymus with hematopoietic progenitors [32, 33]; and kit-ligand (*Kitl*) and interleukin 7 (*Il7*), required in TECs to drive early thymocyte expansion [34, 35]. iTECs retained strong expression of these genes after the coculture period, and no significant differences were observed between the expression levels of these genes in iTECs cultured on different substrates (Fig. 6A*iii-viii*). Of note is that *Dll4, Psmb11, Ctsl1 and Ccl25* all appeared to be expressed more highly in the iTEC after versus before coculture, although this trend reached significance for only *Ctsl1* and *Ccl25* in the Matrigel condition.

We have previously shown that iTECs can produce mTEC-like cells when engrafted under the kidney capsule of recipient mice but that mTEC markers were not present in iTEC monolayers in *in vitro* culture [15]. We therefore looked for *Aire* mRNA transcripts and stained postcoculture iTECs for the mTEC markers cytokeratin 14 (K14), Ulex europaeus agglutinin I (UEA1) and Autoimmune Regulator (AIRE). In keeping with our previous observations, *Aire* expression was undetectable by RT–qPCR in all conditions (Fig. 6A*xi*), and we did not find $K14^+UEA1^+AIRE^+$ cells in any of the conditions tested (Fig. 6B). We did observe $K14^+$ iTECs scattered throughout the monolayers and observed rare $UEA1^+$ iTECs, the frequency of which was increased on gelatin (Fig. S7).

Discussion

We designed and tested a medium/high-throughput assay for the identification of synthetic polymers that support TEC-based cultures able to mediate T-cell production *in vitro*. This assay comprises primary, secondary and tertiary screening elements, which sequentially identify candidate polymers from a large complex polymer library; quantify the capacity of these lead candidates to maintain iTEC and native mouse and human fetal TEC in culture; and test whether the selected polymers maintain iTEC functionality with respect to capacity to support T-cell development in *in vitro* monolayer cultures. The resulting data provide three advances. First, they establish that iTEC can be used to select TEC-relevant compounds in at least some medium/high throughput

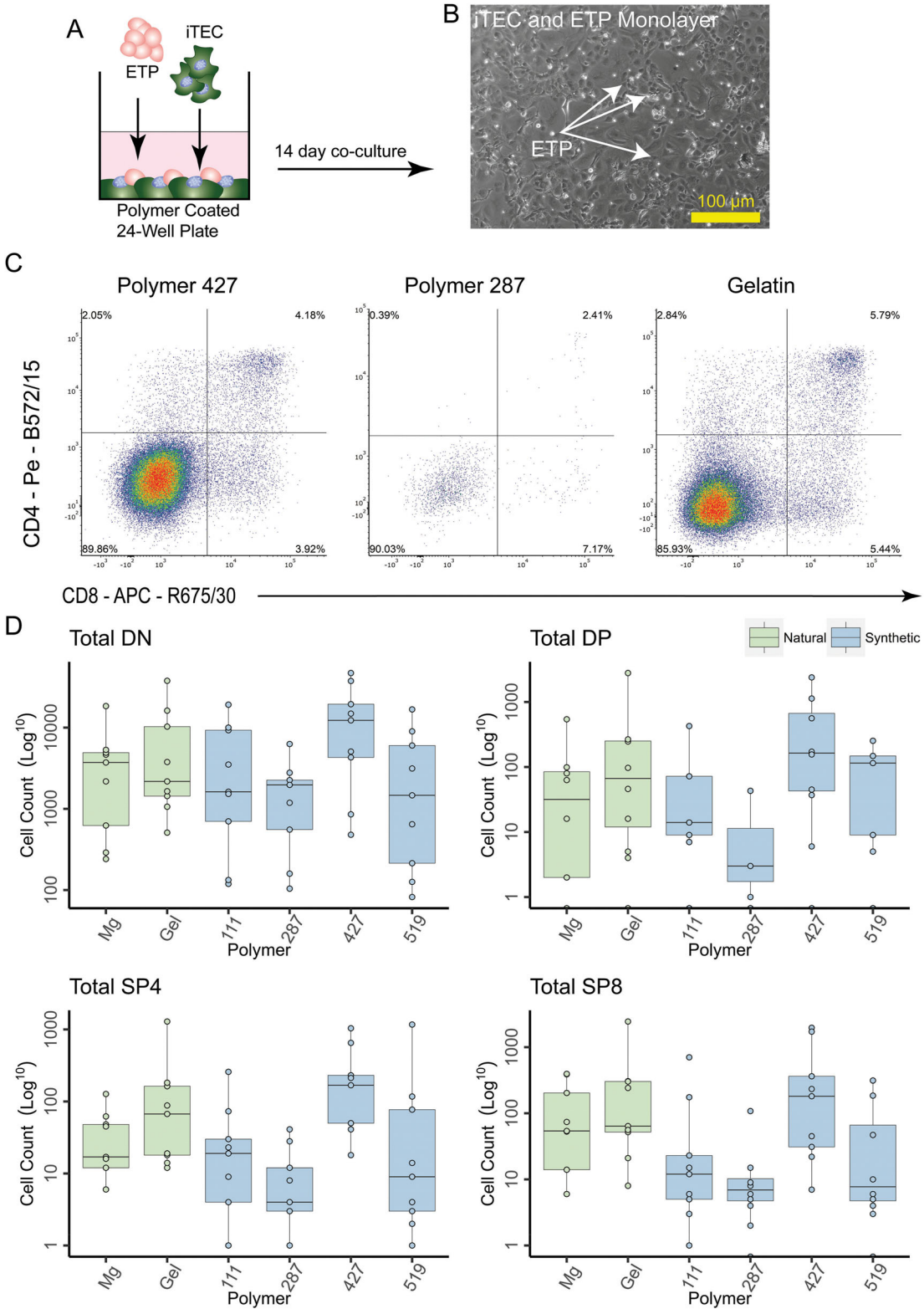

Figure 5. iTECs grown on synthetic polymers, gelatin or Matrigel exhibit equivalent functionality. (A) iTECs were cocultured with adult mouse ETPs in polymer-coated 24-well plates. (B) Representative well after 14 days. (C) Representative CD4/CD8 subset distribution for 14-day iTEC-ETP cocultures in wells coated with polymer ID427 (left panel), polymer ID287 (middle panel) and gelatin (right panel). All plots show live lin$^-$ cells, lin = CD11b, CD11c, Gr-1, Nk1.1, B220, EpCAM and Ter119. (D) Numbers of DN, DP, SP4 and SP8 cells for cells grown in the conditions shown. Green bars, Matrigel and gelatin; Blue bars, synthetic polymers. n = 3 independent biological replicates each with three technical replicates. ANOVA found no significant differences between groups. Mg, Matrigel; Gel, gelatin. Plots formatted as box and whisker.

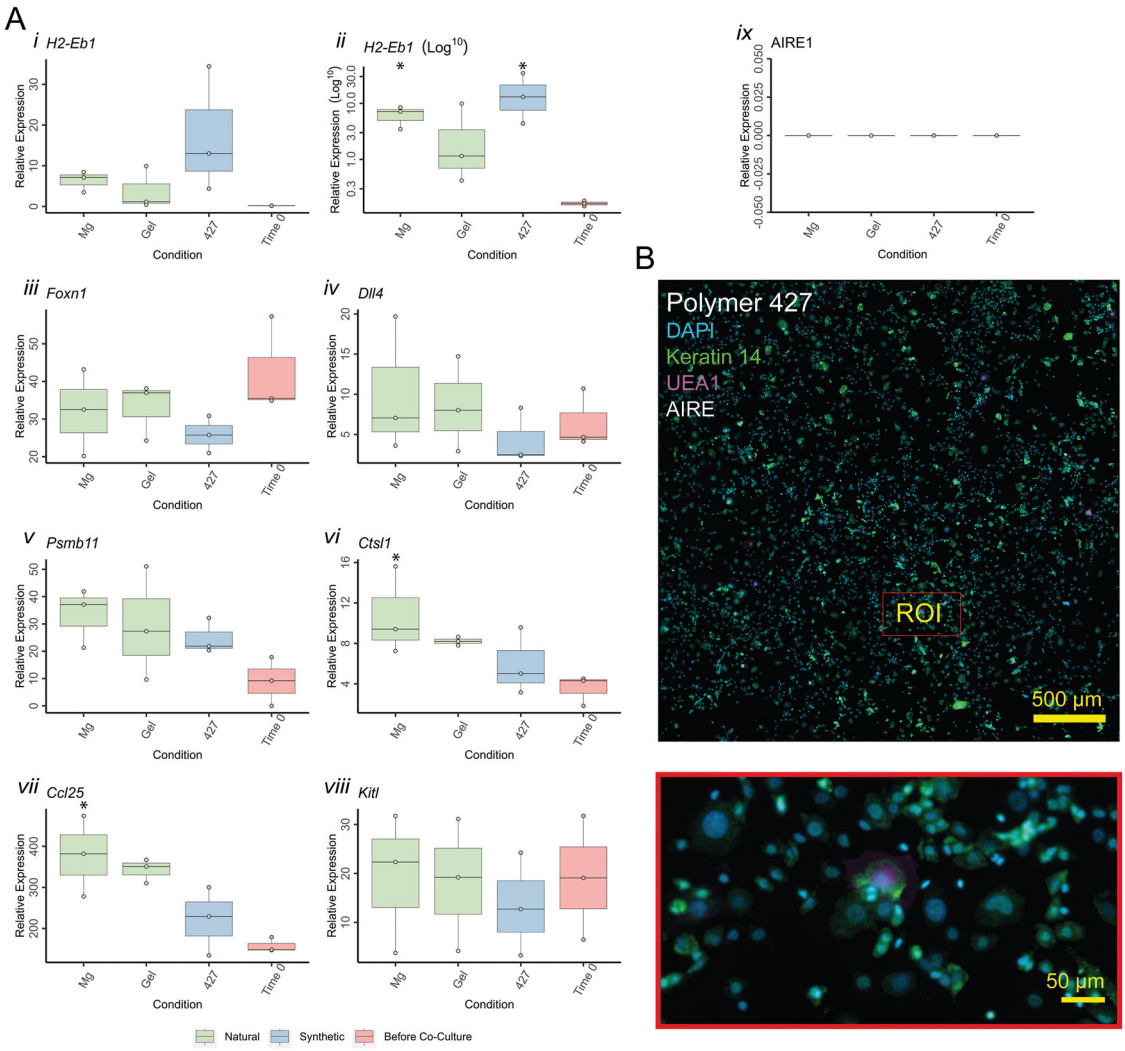

Figure 6. Phenotypic analysis of iTECs cocultured on Polymer ID427. iTECs were cocultured with adult mouse ETPs for 14 days in plates coated with the substrates shown. (Ai-ix) RT–qPCR analysis of the genes shown was performed on iTECs recovered from each condition at the end of the culture period. Aii shows data in Ai after Log10 transformation. (B) After 14 days of coculture, iTECs cultured on polymer ID427 were stained for UEA1$^+$ (magenta), cytokeratin 14$^+$ (green) and AIRE$^+$ (white). Levene's test and Shapiro–Wilk tests established equal variances and normality, respectively. Statistical analysis was performed by one-way ANOVA followed by Tukey's post hoc test. Note that *H2-Eb1*, *Dll1* and *Kitl* were not normally distributed, but only *H2-Eb1* showed a significant difference when $\log_{10}$ transformed. * p value < 0.05 when compared to Time 0. (A, B) n = 3 independent biological replicates, one technical replicate per independent biological replicate. Plots formatted as box and whisker.

screening assays, overcoming the principal bottleneck for further screening related to TEC functionality – namely, the scarcity and hard-to-handle nature of cells of this lineage. Second, they identified four synthetic polymers that support the culture of functional iTECs, as evidenced by the capacity of iTECs to support T-cell development, including SP4 and SP8 cells, in monolayer culture. Third, they show that the synthetic polymer substrates identified using mouse iTEC and native mouse TEC also bind and maintain native human fetal TEC, validating the use of this murine-cell-based assay for selection of polymers suitable for culture of human TEC. Collectively, these data point to the potential of iTECs for use in further screening approaches that address specific aspects of TEC, thymus, and biology. Specific points arising from our study are discussed below.

Strengths and limitations of iTEC as a screening tool

Our study provides a first step toward establishing iTEC as a tool for high-throughput screening for modulators of TEC functionality. As discussed above, the major bottlenecks to this goal are the scarcity and hard-to-handle nature of native TEC and the absence of culture conditions that allow maintenance of functional native TEC in 2D culture. The culture systems that currently best model the thymic microenvironment, FTOC or RFTOC [2, 4], are difficult to upscale because of the technical expertise required and the numbers of fetal thymi/fetal TEC needed for their production. While monolayer OP9-DLL1 and 3D MS5-hDLL1 cell line-based systems circumvent some of these limitations, they do not recapitulate all of the functions of TECs required for T-cell

repertoire development and selection [5, 6], and furthermore, these cell line-based systems cannot provide models for directly testing or screening for modifiers of critical thymus functions that reside in TECs. iTECs represent an alternative to these systems and recapitulate a broader range of TEC characteristics than other cell line-based systems, including expression of the molecular machinery required in TECs to mediate positive and negative selection of the T-cell repertoire [5–15].

We have demonstrated here, to our knowledge for the first time, that iTECs can be used in place of native TECs in at least some *in vitro* screening assays that require high cell numbers and are designed to interrogate TEC functions. Specifically, we have demonstrated that iTECs can be used to select, from a complex library, polymers that can selectively bind and support native mouse and human fetal TECs *in vitro*. Our secondary screen quantified the binding of iTECs and native mouse and human fetal TECs to the polymers selected in the primary screen. This analysis showed very strong concordance between the numbers of iTECs, mouse fetal TECs and human fetal TECs bound by most polymers tested. Polymers identified as having the ability to bind iTEC (ID111, 287, 427 and 519) all bound all three TEC populations in equivalent numbers, while those found to have poor ability to bind iTEC (ID98, 316, 327, 361, 398, 481) bound all three TEC populations poorly.

There was one exception to this pattern, polymer ID531, which bound iTECs and mouse fetal TECs poorly but bound human fetal TECs very strongly. We interpret this as having three possible explanations: since the human fetal TEC data represent n = 1, it may reflect an outlier result that would not carry through on further examination; alternatively, it may reflect interspecies differences in the adhesion molecules or properties of specific adhesion molecules expressed by TEC; and finally, it could represent specific binding by ID531 of a specific TEC subpopulation that was present in the human fetal thymus sample tested but not in iTEC or mouse E14.5 fetal TEC. With respect to this last possibility, thymic medullary compartments are well established by week 11 in human fetal thymus development [36], whereas they are not present in iTEC monolayers [15] and are not well developed in E13.5/E14.5 mouse fetal thymi [37]; therefore, it is possible that polymer ID531 selectively binds mTEC. Exploration of this possibility, however, is beyond the scope of this investigation.

A limitation of the screening approach herein is that we did not perform a side-by-side comparison of iTECs and TECs in the medium/high-throughput primary screen due to practical constraints associated with obtaining sufficient numbers of E13.5/E14.5 fetal TECs. Therefore, it remains possible that in the present study, some polymers that could bind and support native TEC were not identified in the iTEC-based primary screen. Nevertheless, our screening approach enabled the identification of a set of polymers that can bind native TEC as well as or better than Matrigel and gelatin, the substrates currently most commonly used for this purpose. Furthermore, we observed good concordance in the binding of all three TEC populations tested across the polymers tested in the secondary screen. Of note is that twenty-nine of the thirty-two polymers selected in the primary screen and four of the five selected in the secondary screen could not bind and support MEFs, indicating cell-type specificity in the screening steps. In contrast, gelatin and Matrigel support both MEFs and TECs. Overall, our data provide proof of principle for two-stage screening approaches that first use iTEC in a high-throughput primary screen requiring large numbers of input cells and then validate the candidates selected in the primary screen using a low-throughput secondary screen based on native TEC.

We note that even the relatively modest screen we describe required a minimum of three biological replicates each of 2×10^5 iTECs as the cellular input into the primary screen. In pilot experiments, we found that even higher numbers of E14.5 fetal TECs ($>4\times10^5$) were needed to seed each slide. We were unable to obtain this number of E14.5 fetal TECs on a routine basis and thus could not use native fetal TECs in the primary screen (although our laboratory is well established for this type of experiment). This provided the rationale for basing the primary screen on iTEC, since unlimited numbers of iTEC can be generated in the lab. The screen described herein therefore represents an important proof-of-principle, supporting the exploration of further iTEC-based high-throughput screens. In this respect, an important caveat is that FOXN1 is constitutively expressed in iTECs as currently generated [15], regardless of culture conditions; therefore, screening for modulators of FOXN1-dependent functions will require further development of the iTEC reprogramming system.

Identification of synthetic polymers for TEC culture

The screen described herein successfully identified synthetic polymers that bound and supported functional iTECs *in vitro* and bound native mouse and native human fetal TECs. The use of chemically defined synthetic polymers in cell culture has previously been shown to reduce the batch-to-batch variation associated with naturally occurring substrates such as Matrigel, gelatin, or ECM preparations [19]. However, as shown herein and by others, different synthetic polymers bind and support different cell types *in vitro*, necessitating the identification of cell-type-specific polymers [16, 18]. The work presented identifies four polyacrylates that support the culture of iTECs, native mouse fetal TECs and human fetal TECs and shows that culture of iTECs on these polymers did not inhibit iTEC-mediated *in vitro* thymopoiesis, establishing that products such as gelatin and Matrigel can be replaced with defined synthetic polymer preparations for iTEC culture. In this regard, the data shown in Figs. 5C and D show a relatively low level of thymopoiesis in the iTEC-ETP cocultures in all of the conditions tested, and this is markedly different from that demonstrated in our original iTEC publication [15]. As described in the Materials and Methods, we have changed the reprogramming protocol since our original publication; however, we have shown that iTECs generated using our current reprogramming protocol support T-cell development in a very similar

fashion to that originally shown ([15]; see Fig. S2) when cultured under the conditions originally described. In our original paper, we used DN1 cells isolated from E14.5 thymi for the coculture experiments, whereas for the experiments shown in Figs. 5C and D, we used ETPs harvested from adult mice. Since the proliferative capacity of ETPs is known to change with age, this likely explains the differences observed [38, 39].

Our findings strongly suggest that culture of iTECs on polymer ID427 increases the level of expression in iTECs of the MHCII gene *H2-Eb1* compared to expression in iTECs cultured on the natural substrate Matrigel, and iTECs cultured on all of the polymers tested expressed the cTEC-specific antigen processing machinery required for shaping repertoire selection at least as well as iTECs cultured on Matrigel or gelatin. Collectively, these data indicate that iTECs cultured on polymer ID427 should support positive selection of SP4 as well as SP8 thymocytes. These findings also raise the issue of the mechanism through which MHCII expression is increased in iTECs upon coculture. Synthetic polymers are likely to mediate cellular adhesion and support cell maintenance/or growth via a variety of mechanisms, including by binding and potentially changing the bioavailability of specific growth factors. Identification of synthetic polymers that specifically bind TEC points to the use of these polymers, in conjunction with mass spectrometry, as tools for providing insight into the regulation of TEC functionalities such as the regulation of MHCII expression. Further work is required to explore this possibility; we note that the use of synthetic polymers as substrates for TEC culture is not of itself expected to overcome current limitations to culturing functional *ex vivo* TECs. As a final point, the screen described herein was also informative with respect to the transition from MEFs to iTECs. We observed very little overlap in polymer binding between the parental MEFs and the reprogrammed iTECs, establishing that iTECs and MEFs have distinct adhesion profiles, with iTECs acquiring a profile that mimicked that of native TECs, at least with respect to the ability to bind polymers within this library.

Conclusion

Collectively, our data demonstrate that mouse iTECs recapitulate the TEC phenotype sufficiently well to be used in an assay requiring large numbers of TECs that could not otherwise be performed. This is exemplified by the three-tier screening assay described herein, through which we have identified synthetic polymer ID427 as suitable for replacing naturally occurring materials in iTEC culture protocols. Taken together with our previous findings demonstrating the ability of iTECs to form a self-organized thymic organoid upon transplantation and to mediate T-cell lineage commitment and development *in vitro* [15], our data establish the potential for the development of further iTEC-based high-throughput assays related to TEC biology, for instance, to screen for pharmaceutical compounds that augment or explore TEC regulation and function. Currently, there is clinical interest in promoting thymic rebound after myeloablative hematopoietic stem cell transplantation, but efforts in this direction currently lack a suitable *in vitro* model system for large-scale drug discovery [40]. Our data highlight the potential suitability of iTEC for this role.

Materials and methods

Mice

C57BL/6 mice were used for isolation of fetal TECs. For timed matings, noon of the day of the vaginal plug was taken as day 0.5 of embryonic development (E0.5). Rosa26-CreERT2 [41] and *Rosa26*$^{CAG\text{-}Foxn1\text{-}IRES\text{-}GFP}$ (iFoxn1) [15] mice were as described. All animals were housed and bred at the CRM animal facility. All experimental procedures were conducted in compliance with the Home Office Animals (Scientific Procedures) Act 1986 under project license PEEC9E359 to V. Wilson. The primers used for genotyping are shown in Table S1. All controls were littermates unless otherwise stated.

Human tissue

The first trimester human fetus was obtained following elective medical termination of pregnancy and was morphologically normal. Ethical approval for the use of human fetal tissue in these studies was granted by the Lothian Research Ethics Committee. Consent was obtained in writing, and the tissue was anonymized before being made available for research. The embryo was aged at wk 11 post fertilization according to the standard head/rump measurement, and the Carnegie stage was determined [42, 43].

MEFs

MEFs were prepared from E13.5 embryos as previously described [15] (see also Supporting Information). Each MEF culture was genotyped for the iFoxn1 and ROSA26-CreERT2 alleles. *Rosa26*$^{CreERT2/CAG\text{-}Foxn1\text{-}IRES\text{-}GFP}$ (iFoxn1) and *Rosa26*$^{CreERT2/+}$ (Control) MEFs were used for all experiments.

Induced thymic epithelial cells (iTECs)

iFoxn1 or control MEFs were thawed and seeded directly into a T75 flask in iTEC medium (see Supporting Information) and then prepared as previously described [15] with the following changes from the original protocol: 0.1 μM 4OHT was added to freshly replated iFoxn1 MEFs at day 0 (2.5×10^6 cells per T150) and washed out after 48 hours. The medium was then changed every 2–3 days until day 18, when GFP$^+$ cells (iTECs) were harvested by flow cytometric cell sorting prior to use (sort gates shown in Fig. S1). See Supporting Information for details. iTECs produced by

this protocol were validated by phenotypic and functional analyses as shown in Fig. S2.

iTEC-based reaggregate thymic organ cultures and reaggregate fetal thymic organ cultures were established as previously described [15]. Thymus dissociation was performed as described in the Supporting Information.

Polymer library preparation

The polyacrylates in the library were each synthesized by free radical polymerization, and in the case of polymers containing glycidyl methacrylate, they were reacted with an amine-based monomer, as described [19] (Table S4).

Polymer arrays

Polymer arrays were generated and utilized as described in the Supplementary Information. In all screening experiments, iTECs and TECs were cultured in iTEC medium. All coculture experiments used 'coculture medium'.

Flow cytometry

Cells were processed for flow cytometric sorting and analysis as previously described [15, 44] and in adherence to the guidelines on flow cytometry and cell sorting in immunological studies [45]. See Supplementary Information for detailed protocol for each population. Sorting was performed using a BD FACS Aria II or Fusion running FACS Diva 4.1 (BD Biosciences), and analysis was performed on a Novocyte running NovoExpress 1.3.0 (ACEA). All postacquisition analyses were performed with FCSexpress 6 (De Novo Software).

Immunohistochemistry

Immunohistochemistry was performed as described [46]. Appropriate isotype and negative controls were included in all experiments. Immunofluorescence on the microarrays was detected using Nikon 50i (Nikon), SP8 confocal (Leica Microsystem, GmbH) or Axio Observer (Zeiss) microscopes. Images presented are of single optical sections. Fiji software [47] was used to process images for manual cell counting of the microarray. For detection of immunofluorescence on the focused arrays, Operetta and Columbus software (Perkin Elmer) was used for automated image capture and analysis, respectively.

Antibodies

The antibodies used for flow cytometry are listed in Tables S2, S3, and S6, and those used for immunohistochemistry are listed in Table S5.

Culture media

Culture media were as in the Supplementary Information.

Statistics

Statistical analyses were performed in R; the tests used are described in the figure legends. Levene's and Shapiro–Wilk tests were used to establish equal variances and normality of residuals, respectively. For all tests, the alpha level was taken as 0.05. Sample sizes were at least n = 3 except where indicated. For all analyses, n represents the number of independent biological experiments. No statistical method was used to predetermine sample size, the experiments were not randomized, and the investigators were not blinded to allocation during experiments and outcome assessment. There were no limitations to the repeatability of the experiments. No samples were excluded from the analysis. Graphs were prepared using the R package ggplot2 [48] and depict box plots, with the exception of the human data where n = 1; therefore, the data are displayed as a dot plot.

Acknowledgments: We thank C. Cryer and F. Rossi (CRM, University of Edinburgh) for cell sorting, E. O'Duibhir and B. Vernay (CRM, University of Edinburgh) for imaging, and the BRF staff for animal care. The research leading to these results received funding from the UKRI-Biotechnology and Biological Sciences Research Council through an industrial CASE studentship award (CCB, PR), the UKRI-Medical Research Council through an MRC-DTP studentship (JS), the European Union Seventh Framework Programme (FP7/2007-2013) collaborative project ThymiStem under grant agreement number 602587 (CCB, TH), and the Wellcome Trust collaborative award 211944/Z/18/Z (CCB, TH, PR). For the purpose of open access, the author has applied a CC-BY public copyright licence to any Author Accepted Manuscript version arising from this submission.

Conflict of interest: The authors declare no commercial or financial conflicts of interest.

Author contributions: P.R. and T.H. were associated with conception and design, collection and assembly of data, data analysis and interpretation, and manuscript writing. S.V. and C.D. provided study material. J.S. was associated with collection and assembly of data, and data analysis and interpretation. M.B. was associated with conception and design, data analysis and interpretation, and final approval of manuscript. C.C.B. was associated with conception and design, financial support, provision of study material, data analysis and interpretation, manuscript writing, and final approval of manuscript.

Data availability statement: The data that support the findings of this study are available from the corresponding author upon reasonable request.

Peer review: The peer review history for this article is available at https://publons.com/publon/10.1002/eji.202249934

References

1 **Abramson, J. and Anderson, G.**, Thymic Epithelial Cells. *Annu. Rev. Immunol.* 2017. **35**: 85–118.

2 **Anderson, G., Jenkinson, E. J., Moore, N. C. and Owen, J. J. T.**, MHC class II positive epithelium and mesenchyme cells are both required for T-cell development in the thymus. *Nature.* 1993. **362**: 70–73.

3 **Jenkinson, E. J. and Owen, J. J.**, T-cell differentiation in thymus organ cultures. *Semin. Immunol.* 1990. **2**: 51–58.

4 **Sheridan, J. M., Taoudi, S., Medvinsky, A. and Blackburn, C. C.**, A novel method for the generation of reaggregated organotypic cultures that permits juxtaposition of defined cell populations. *Genesis.* 2009. **47**: 346–351.

5 **Seet, C. S., He, C., Bethune, M. T., Li, S., Chick, B., Gschweng, E. H., Zhu, Y. et al.**, Generation of mature T cells from human hematopoietic stem and progenitor cells in artificial thymic organoids. *Nat. Methods.* 2017. **14**: 521–530.

6 **Schmitt, T. M. and Zuniga-Pflucker, J. C.**, Induction of T-cell development from hematopoietic progenitor cells by delta-like-1 in vitro. *Immunity.* 2002. **17**: 749–756.

7 **Gommeaux, J., Gregoire, C., Nguessan, P., Richelme, M., Malissen, M., Guerder, S., Malissen, B. et al.**, Thymus-specific serine protease regulates positive selection of a subset of CD4+ thymocytes. *Eur. J. Immunol.* 2009. **39**: 956–964.

8 **Honey, K., Nakagawa, T., Peters, C. and Rudensky, A.**, Cathepsin L regulates CD4+ T-cell selection independently of its effect on invariant chain: a role in the generation of positively selecting peptide ligands. *J. Exp. Med.* 2002. **195**: 1349–1358.

9 **Murata, S., Sasaki, K., Kishimoto, T., Niwa, S., Hayashi, H., Takahama, Y. and Tanaka, K.**, Regulation of CD8+ T-cell development by thymus-specific proteasomes. *Science.* 2007. **316**: 1349–1353.

10 **Nakagawa, T., Roth, W., Wong, P., Nelson, A., Farr, A., Deussing, J., Villadangos, J. A. et al.**, Cathepsin L: critical role in Ii degradation and CD4 T-cell selection in the thymus. *Science*. 1998. **280**: 450–453.

11 **Takaba, H., Morishita, Y., Tomofuji, Y., Danks, L., Nitta, T., Komatsu, N., Kodama, T. et al.**, Fezf2 Orchestrates a Thymic Program of Self-Antigen Expression for Immune Tolerance. *Cell*. 2015. **163**: 975–987.

12 **Anderson, M. S., Venanzi, E. S., Klein, L., Chen, Z., Berzins, S. P., Turley, S. J., von Boehmer, H. et al.**, Projection of an immunological self shadow within the thymus by the aire protein. *Science.* 2002. **298**: 1395–1401.

13 **Anderson, M. S. and Su, M. A.**, AIRE expands: new roles in immune tolerance and beyond. *Nat. Rev. Immunol.* 2016. **16**: 247–258.

14 **Nitta, T., Murata, S., Sasaki, K., Fujii, H., Ripen, A. M., Ishimaru, N., Koyasu, S. et al.**, Thymoproteasome shapes immunocompetent repertoire of CD8+ T cells. *Immunity.* 2010. **32**: 29–40.

15 **Bredenkamp, N., Ulyanchenko, S., O'Neill, K. E., Manley, N. R., Vaidya, H. J. and Blackburn, C. C.**, An organized and functional thymus generated from FOXN1-reprogrammed fibroblasts. *Nat. Cell Biol.* 2014. **16**: 902–908.

16 **Hay, D. C., Pernagallo, S., Diaz-Mochon, J. J., Medine, C. N., Greenhough, S., Hannoun, Z., Schrader, J. et al.**, Unbiased screening of polymer libraries to define novel substrates for functional hepatocytes with inducible drug metabolism. *Stem. Cell Res.* 2011. **6**: 92–102.

17 **Lucendo-Villarin, B., Cameron, K., Szkolnicka, D., Travers, P., Khan, F., Walton, J. G., Iredale, J. et al.**, Stabilizing hepatocellular phenotype using optimized synthetic surfaces. *J. Vis. Exp.* 2014.: 51723.

18 **Nakamura, A., Wong, Y. F., Venturato, A., Michaut, M., Venkateswaran, S., Santra, M., Gonçalves, C. et al.**, Long-term feeder-free culture of human pancreatic progenitors on fibronectin or matrix-free polymer potentiates beta cell differentiation. *Stem. Cell Reports.* 2022. **17**: 1215–1228.

19 **Tourniaire, G., Collins, J., Campbell, S., Mizomoto, H., Ogawa, S., Thaburet, J. F. and Bradley, M.**, Polymer microarrays for cellular adhesion. *Chem. Commun. (Camb.)* 2006.: 2118–2120.

20 **Poznansky, M. C., Evans, R. H., Foxall, R. B., Olszak, I. T., Piascik, A. H., Hartman, K. E., Brander, C. et al.**, Efficient generation of human T cells from a tissue-engineered thymic organoid. *Nature Biotech.* 2000. **18**: 729–734.

21 **Campinoti, S., Gjinovci, A., Ragazzini, R., Zanieri, L., Ariza-McNaughton, L., Catucci, M., Boeing, S. et al.**, Reconstitution of a functional human thymus by postnatal stromal progenitor cells and natural whole-organ scaffolds. *Nat. Commun.* 2020. **11**: 6372.

22 **Chung, B., Montel-Hagen, A., Ge, S., Blumberg, G., Kim, K., Klein, S., Zhu, Y. et al.**, Engineering the human thymic microenvironment to support thymopoiesis in vivo. *Stem. Cells.* 2014. **32**: 2386–2396.

23 **Fan, Y., Tajima, A., Goh, S. K., Geng, X., Gualtierotti, G., Grupillo, M., Coppola, A. et al.**, Bioengineering Thymus Organoids to Restore Thymic Function and Induce Donor-Specific Immune Tolerance to Allografts. *Mol. Ther.* 2015. **23**: 1262–1277.

24 **Hun, M., Barsanti, M., Wong, K., Ramshaw, J., Werkmeister, J. and Chidgey, A. P.**, Native thymic extracellular matrix improves in vivo thymic organoid T-cell output, and drives in vitro thymic epithelial cell differentiation. *Biomaterials.* 2017. **118**: 1–15.

25 **Asnaghi, M. A., Barthlott, T., Gullotta, F., Strusi, V., Amovilli, A., Hafen, K., Srivastava, G. et al.**, Thymus Extracellular Matrix-Derived Scaffolds Support Graft-Resident Thymopoiesis and Long-Term In Vitro Culture of Adult Thymic Epithelial Cells. *Adv. Funct. Mater.* 2021. **31**: 2010747.

26 **Bortolomai, I., Sandri, M., Draghici, E., Fontana, E., Campodoni, E., Marcovecchio, G. E., Ferrua, F. et al.**, Gene Modification and Three-Dimensional Scaffolds as Novel Tools to Allow the Use of Postnatal Thymic Epithelial Cells for Thymus Regeneration Approaches. *Stem. Cells Transl. Med.* 2019. **8**: 1107–1122.

27 **Duffy, C. R. E., Zhang, R., How, S. E., Lilienkampf, A., Tourniaire, G., Hu, W., West, C. C. et al.**, A high-throughput polymer microarray approach for identifying defined substrates for mesenchymal stem cells. *Biomater. Sci.* 2014. **2**: 1683–1692.

28 **Zhang, Y., Venkateswaran, S., Higuera, G. A., Nath, S., Shpak, G., Matray, J., Fratila-Apachitei, L. E. et al.**, Synthetic Polymers Provide a Robust Substrate for Functional Neuron Culture. *Adv. Healthc. Mater.* 2020. **9**: e1901347.

29 **Koch, U., Fiorini, E., Benedito, R., Besseyrias, V., Schuster-Gossler, K., Pierres, M., Manley, N. R. et al.**, Delta-like 4 is the essential, nonredundant ligand for Notch1 during thymic T-cell lineage commitment. *J. Exp. Med.* 2008. **205**: 2515–2523.

30 **Hozumi, K., Mailhos, C., Negishi, N., Hirano, K., Yahata, T., Ando, K., Zuklys, S. et al.**, Delta-like 4 is indispensable in thymic environment specific for T-cell development. *J. Exp. Med.* 2008. **205**: 2507–2513.

31 **Murata, S., Takahama, Y., Kasahara, M. and Tanaka, K.**, The immunoproteasome and thymoproteasome: functions, evolution and human disease. *Nat. Immunol.* 2018. **19**: 923–931.

32 **Calderon, L. and Boehm, T.**, Three chemokine receptors cooperatively regulate homing of hematopoietic progenitors to the embryonic mouse thymus. *Proc. Natl. Acad. Sci. U S A.* 2011. **108**: 7517–7522.

33 **Bajoghli, B., Aghaallaei, N., Hess, I., Rode, I., Netuschil, N., Tay, B. H., Venkatesh, B. et al.**, Evolution of genetic networks underlying the emergence of thymopoiesis in vertebrates. *Cell.* 2009. **138**: 186–197.

34 **Buono, M., Facchini, R., Matsuoka, S., Thongjuea, S., Waithe, D., Luis, T. C., Giustacchini, A. et al.**, A dynamic niche provides Kit ligand in a stage-specific manner to the earliest thymocyte progenitors. *Nat. Cell Biol.* 2016. **18**: 157–167.

35 **Shitara, S., Hara, T., Liang, B., Wagatsuma, K., Zuklys, S., Hollander, G. A., Nakase, H. et al.**, IL-7 produced by thymic epithelial cells plays a major role in the development of thymocytes and TCRgammadelta+ intraepithelial lymphocytes. *J. Immunol.* 2013. **190**: 6173–6179.

36 **Farley, A. M., Morris, L. X., Vroegindeweij, E., Depreter, M. L., Vaidya, H., Stenhouse, F. H., Tomlinson, S. R. et al.**, Dynamics of thymus organogenesis and colonization in early human development. *Development.* 2013. **140**: 2015–2026.

37 **Klug, D. B., Carter, C., Gimenez-Conti, I. B. and Richie, E. R.**, Cutting edge: thymocyte-independent and thymocyte-dependent phases of epithelial patterning in the fetal thymus. *J. Immunol.* 2002. **169**: 2842–2845.

38 **Min, H., Montecino-Rodriguez, E. and Dorshkind, K.**, Reduction in the developmental potential of intrathymic T-cell progenitors with age. *J. Immunol.* 2004. **173**: 245–250.

39 **Berent-Maoz, B., Montecino-Rodriguez, E., Fice, M., Casero, D., Seet, C. S., Crooks, G. M., Lowry, W. et al.**, The expansion of thymopoiesis in neonatal mice is dependent on expression of high mobility group a 2 protein (Hmga2). *PLoS One.* 2015. **10**: e0125414.

40 **Chaudhry, M. S., Velardi, E., Dudakov, J. A. and van den Brink, M. R.**, Thymus: the next (re)generation. *Immunol. Rev.* 2016. **271**: 56–71.

41 **Hameyer, D., Loonstra, A., Eshkind, L., Schmitt, S., Antunes, C., Groen, A., Bindels, E. et al.**, Toxicity of ligand-dependent Cre recombinases and generation of a conditional Cre deleter mouse allowing mosaic recombination in peripheral tissues. *Physiol. Genomics.* 2007. **31**: 32–41.

42 **Gasser, R. F.**, Atlas of human embryos: Harper & Row 1975.

43 **O'Rahilly, R. and Muller, F.**, *Developmental stages in human embryos: including a revision of Streeter's Horizons and a survey of the Carnegie collection*. Washington D.C.: Carnegie Institution of Washington. 1987.

44 **Nowell, C. S., Bredenkamp, N., Tetelin, S., Jin, X., Tischner, C., Vaidya, H., Sheridan, J. M. et al.**, Foxn1 regulates lineage progression in cortical and medullary thymic epithelial cells but is dispensable for medullary sublineage divergence. *PLoS Genet.* 2011. **7**: e1002348.

45 **Cossarizza, A., Chang, H. D., Radbruch, A., Abrignani, S., Addo, R., Akdis, M., Andrä, I. et al.**, Guidelines for the use of flow cytometry and cell sorting in immunological studies (third edition). *Eur. J. Immunol.* 2021. **51**: 2708–3145.

46 **Gordon, J., Wilson, V. A., Blair, N. F., Sheridan, J., Farley, A., Wilson, L., Manley, N. R. et al.**, Functional evidence for a single endodermal origin for the thymic epithelium. *Nat. Immunol.* 2004. **5**: 546–553.

47 **Schindelin, J., Arganda-Carreras, I., Frise, E., Kaynig, V., Longair, M., Pietzsch, T., Preibisch, S. et al.**, Fiji: an open-source platform for biological-image analysis. *Nat. Methods.* 2012. **9**: 676–682.

48 **Wickham, H.**, *ggplot2: Elegant Graphics for Data Analysis*. New York: Springer-Verlag; 2016.

Abbreviations: **DN:** $CD4^-CD8^-$ Double Negative Thymocyte · **DP:** $CD4^+CD8^+$ Double-Positive Thymocyte · **E,:** Day of Embryonic Development · **ECM:** Extracellular Matrix · **ETP:** Early thymocyte progenitor · **iTEC:** induced Thymic Epithelial Cells · **K14:** Cytokeratin 14 · **MEFs:** Murine Embryonic Fibroblasts · **panK:** Pan-cytokeratin · **SP4:** $CD4^+CD8^-$ Single Positive Thymocyte · **SP8:** $CD4^-CD8^+$ Single Positive Thymocyte · **TEC:** Thymic Epithelial Cell

Full correspondence: C. Clare Blackburn, Centre for Regenerative Medicine, Institute for Stem Cell Research, School of Biological Sciences, University of Edinburgh, 5 Little France Drive, Edinburgh EH16 4UU.
e-mail: c.blackburn@ed.ac.uk

Received: 5/4/2022
Revised: 7/11/2022
Accepted: 13/1/2023
Accepted article online: 16/1/2023